

# Spectral monitoring of RX J1856.5-3754 with XMM-Newton

## Analysis of EPIC-pn data

N. Sartore<sup>1</sup>, A. Tiengo<sup>1,2</sup>, S. Mereghetti<sup>1</sup>, A. De Luca<sup>1,2,3</sup>, R. Turolla<sup>4,5</sup>, and F. Haberl<sup>6</sup>

<sup>1</sup> INAF - Istituto di Fisica Spaziale e Fisica Cosmica, via E. Bassini 15, 20133, Milano, Italy e-mail: sartore@iasf-milano.inaf.it

<sup>2</sup> IUSS - Istituto Universitario di Studi Superiori, viale Lungo Ticino Sforza 56, 27100, Pavia, Italy

<sup>3</sup> INFN - Istituto Nazionale di Fisica Nucleare, sezione di Pavia, via A. Bassi 6, 27100, Pavia, Italy

<sup>4</sup> Dipartimento di Fisica e Astronomia, Università di Padova, via Marzolo 8, 35131, Padova, Italy

<sup>5</sup> Mullard Space Science Laboratory, University College London, Holmbury St. Mary, Dorking, Surrey, RH5 6NT, UK

<sup>6</sup> Max-Planck-Institut für extraterrestrische Physik, Giessenbachstraße, 85748 Garching bei München, Germany

Received ...; accepted ...

### ABSTRACT

Using a large set of XMM-Newton observations we searched for long term spectral and flux variability of the isolated neutron star RX J1856.5-3754 in the time interval from April 2002 to October 2011. This is the brightest and most extensively observed source of a small group of nearby, thermally emitting isolated neutron stars, of which at least one member (RX J0720.4-3125, see e.g. Hohle et al., 2010) has shown long term variability. A detailed analysis of the data obtained with the EPIC-pn camera in the 0.15 – 1.2 keV energy range reveals only small variations in the temperature derived with a single blackbody fit (of the order of  $\sim 1\%$  around an average value of  $kT^\infty \sim 61$  eV). Such variations appear to be correlated with the position of the source on the detector and can be ascribed to an instrumental effect, most likely a spatial dependence of the channel to energy relation. For the sampled instrumental coordinates, we quantify this effect as variations of  $\sim 4\%$  and  $\sim 15$  eV in the gain slope and offset, respectively. Selecting only a homogeneous subset of observations, with the source imaged at the same detector position, we find no evidence for spectral or flux variations of RX J1856.5-3754 from March 2005 to present-day, with limits of  $\Delta kT^\infty < 0.5\%$  and  $\Delta f_X < 3\%$  (0.15 – 1.2 keV range), with  $3\sigma$  confidence. A slightly higher temperature ( $kT^\infty \sim 61.5$  eV, compared to the average value  $kT^\infty \sim 61$  eV) was instead measured in April 2002. If this difference is not of instrumental origin, it implies a rate of variation  $\sim -0.15$  eV yr<sup>-1</sup> between April 2002 and March 2005. The high-statistics source spectrum from the selected observations is best fitted with the sum of two blackbody models, with temperatures  $kT_h^\infty = 62.4^{+0.6}_{-0.4}$  eV and  $kT_s^\infty = 38.9^{+4.9}_{-2.9}$  eV, which can also account for the flux seen in the optical band. No significant narrow or broad spectral features are detected, with upper limits of  $\sim 6$  eV on their equivalent width.

**Key words.** Stars: neutron, Stars: Individual: RX J1856.5-3754

## 1. INTRODUCTION

RX J1856.5-3754 (J1856 hereafter) is the prototype of the so-called XDINSs, i.e. the seven X-ray Dim Isolated Neutron Stars discovered by the ROSAT satellite (e.g. Walter et al. 1996, see also Haberl 2007; Turolla 2009 for reviews). These are nearby,  $d \lesssim 300$  pc, radio-quiet isolated neutron stars characterized by thermal spectra, with temperatures<sup>1</sup>  $kT^\infty \sim 50 - 100$  eV and luminosities  $L_X \sim 10^{31} - 10^{32}$  erg s<sup>-1</sup>. Six out of the seven XDINSs exhibit broad spectral features at energies between 270 and 700 eV, with equivalent widths of several tens of eV, interpreted as proton cyclotron lines or atomic transitions in strong magnetic fields,  $B \sim 10^{13}$  G. Spin periods of the XDINSs are in the 3–12 s range and, assuming magneto-dipole braking, their measured spin-down rates, of  $\sim 10^{-14} - 10^{-13}$  s s<sup>-1</sup>, imply magnetic fields  $B \sim 10^{13} - 10^{14}$  G, in broad agreement with those inferred from the spectral features. All XDINSs have very faint optical/UV counterparts,  $m_V \sim 26 - 27$ : the optical/UV flux exceeds that expected from the Rayleigh-Jeans tail of the X-ray blackbody (BB, see e.g. Kaplan et al., 2011).

Intriguingly, the second brightest XDINS, RX J0720.4-3125 (J0720 hereafter) showed significant long term variations of its

spectral properties (Hohle et al., 2010, and references therein). The nature of these changes is still under debate and can possibly be related to a precession of its spin axis (e.g. Haberl et al., 2006) or to a glitch-like episode (van Kerkwijk et al., 2007). Another interesting fact is that XDINSs share some of their properties with magnetars. In particular, their spin periods fall in the same range, while the magnetic fields of XDINSs are intermediate between those of magnetars,  $B \sim 10^{14} - 10^{15}$  G, and normal pulsars,  $B \sim 10^{11} - 10^{13}$  G. Also, XDINSs seem to be older than magnetars, with spindown ages of  $\sim 10^5 - 10^6$  years against  $\sim 10^3 - 10^5$  years (e.g. Mereghetti, 2008). These similarities suggest a possible evolutionary link between the two classes of isolated neutron stars (INSs).

J1856 has the lowest pulsed fraction,  $\sim 1\%$  (Tiengo & Mereghetti, 2007), and the weakest magnetic field,  $B \sim 1.5 \times 10^{13}$  G (van Kerkwijk & Kaplan, 2008) among known XDINSs. Being the brightest,  $f_X \sim 1.5 \times 10^{-11}$  erg s<sup>-1</sup> cm<sup>-2</sup> and closest of the category,  $d = 123^{+11}_{-15}$  pc (e.g. Walter et al., 2010), it stands among the best candidates to probe the mass and radius of a neutron star, which in turn would be of paramount importance to constrain the equation of state (EOS) of matter at nuclear densities. Analyzing the data from a 57 ks XMM-Newton observation and a  $\sim 500$  ks observation

<sup>1</sup> measured by an observer at infinity.

by *Chandra*, Burwitz et al. (2003) suggested that atmosphere models with heavy elements can be ruled out, given the lack of any spectral features. Also, they ruled out non-magnetic and fully ionized hydrogen atmosphere models, since both would over-predict the optical flux. On the other hand, they found that the broadband (optical + X-ray) spectrum is well fitted by a two component BB, where the hotter component,  $kT_X^\infty \simeq 63.5$  eV ( $R_X^\infty \simeq 4.4 (d/120 \text{ pc}) \text{ km}$ ), is responsible for the X-ray emission while the cold component,  $kT_{opt} < 33$  eV ( $R_{opt}^\infty > 17 (d/120 \text{ pc}) \text{ km}$ ), accounts only for the optical emission. Alternative models, like emission from condensed matter surface (Lai, 2001; Turolla et al., 2004), or partially ionized hydrogen atmospheres (Ho et al., 2007) cannot be ruled out.

Thanks to its bright and presumably steady emission, J1856 has been targeted routinely for calibration purposes by XMM-Newton in the last decade. The large amount of collected data allows us to precisely characterize its spectral evolution on time scales from months to  $\sim 10$  years. At the same time, the stability of the detectors on board XMM-Newton in the same time-frame can be scrutinized as well, as done with the data taken before 2006 in Haberl (2007). Here we report on the analysis of all XMM-Newton observations of J1856 performed so far in imaging mode with the EPIC-pn camera (Strüder et al., 2001) on board XMM-Newton. The reduction and the analysis of the data is described in Section 2. Results are also illustrated in Section 2. We constrain the detector stability and obtain an upper limit for the spectral variations of the star and compare it with those of other isolated neutron stars reported in the literature. A discussion on the astrophysical implications of these results is also given (Section 3).

## 2. DATA REDUCTION AND SPECTRAL ANALYSIS

We use all imaging data collected with the EPIC-pn camera from April 2002 to October 2011. Data from the two EPIC-MOS detectors are not considered in this analysis because the MOS effective area at soft X-ray energies is much smaller than that of the pn and the MOS cameras are known to be less stable on long term (Read et al., 2006). Table 1 reports the date, identification number, net exposure time, and number of background-subtracted counts of J1856 for each observation. All observations were performed in Small Window mode with the thin filter. Raw data are processed with the XMM-Newton science analysis package (SAS) v11.0, using the *eproc* pipeline. We then build light curves above 10 keV, with bin size of 100 s, in order to identify soft proton flares. Based on these light curves, we clean the data by removing time intervals with count rate higher than  $4\sigma$  above the mean rate. Source spectra are then extracted from a circular region of  $30''$  radius, selecting only single pixel events (i.e. PATTERN=0 in the *xmmselect* task), in order to obtain event lists of the highest possible quality. The extracted spectra are binned in order to have at least 30 counts per bin. The spectral analysis is performed with XSPEC 12 (Arnaud, 1996), selecting photon energies in the 0.15 – 1.2 keV range.

We perform a simultaneous fit of all the 20 spectra with a single absorbed BB, using a *phabs\*bbbodyrad* model and adopting the abundances of Anders & Grevesse (1989). The true spectra of XDINSs can be more complex than a single BB. However, we are interested in relative variations in the emission of J1856. Thus, we rely on the parameters of the single BB in order to quantify these variations. The best fit gives a BB temperature  $kT^\infty = 61.30 \pm 0.04$  eV, and a column density  $N_H = (5.84 \pm 0.04) \times 10^{19} \text{ cm}^{-2}$  ( $\chi_\nu^2 = 1.78$  with 2784 degrees of freedom). The residuals show large systematic deviations, espe-

cially above  $\sim 0.5$  keV (Fig. 1, upper panel), which change from observation to observation, indicating that some of the spectral parameters vary between different observations. Therefore, we repeat the spectral fit leaving the BB temperature and normalization as free parameters for each observation. In this case we obtain a better  $\chi_\nu^2 = 1.37$  with 2746 degrees of freedom. The resulting parameters are shown in Fig. 2 (panels *a*, *b*, *c*). The fit of the 20 spectra with the column density as free parameter, and a unique temperature and normalization for all observations, is not as good as the previous one,  $\chi_\nu^2 = 1.58$  with 2765 degrees of freedom. The resulting column densities are shown in Fig. 2 (panel *d*). The count rate shows variations of  $\sim 1 - 2$  percent around a mean of  $\sim 7.46 \text{ cts s}^{-1}$ , but with no evidence of a defined trend and without correlation with the BB temperature or normalization. On the other hand, the hydrogen column density is clearly anti-correlated with the count rate (compare panels *a* and *d* in Fig. 2), indicating that the changes in the count rate are mainly determined by differences in the softest spectral band. As already noticed by Stuhlinger et al. (2010), the temperature also shows variations of  $\sim 1 - 2$  percent ( $\sim 1.5 - 2$  eV), which are anti-correlated with the normalization. We note that these variations have a seasonal pattern with a period of  $\sim 12$  months, suggesting that they are likely related to instrumental effects rather than being intrinsic changes of the source emission. To verify this hypothesis we study the relation of the BB temperature with the position of the source centroid on the detector (RAWX and RAWY coordinates). With the exception of the three off-axis observations (observations H, P and Q, which includes the four separate pointings performed in October 2011) and one in an intermediate position (observation F), in most of the observations the source centroid lies in two close but distinct regions of the detector (Fig. 3), one at RAWX $\sim$ 36-37, RAWY $\sim$ 192, and the other one at RAWX $\sim$ 38, RAWY $\sim$ 190 (hereafter ‘soft’ and ‘hard’ region, respectively, according to the relative hardness of their spectra, as outlined below). This is due to the different roll angle of the satellite in the Spring and Fall visibility intervals for the J1856 sky region.

The best fit BB temperature is systematically higher for observations with the source in the ‘hard’ region (upper right and lower left panels of Fig. 3), and in the 3 most extreme off axis observations at RAWY=168, RAWX=16 and RAWX=56. In the pn camera the signal is read independently from each column along the RAWY position. This implies that small inaccuracies in either the gain or the charge transfer inefficiency (CTI) correction along the readout direction could be the underlying cause for the observed spectral differences. Thus we fit again all the spectra with a unique BB model, but this time allowing a variation of the gain parameters. These parameters, *slope* and *offset*, define the relation between the energy scale in the response matrix of each observation with respect to that of an observation taken as reference:  $E'_i = E / \text{slope}_i - \text{offset}_i$ . We assume the spectrum of the first observation (observation A) as reference, i.e. we fix its *slope* and *offset* at 1 and 0, respectively. In this case we obtain  $\chi_\nu^2 = 1.32$  with 2746 degrees of freedom, with a net reduction of the scatter of fit residuals for all spectra (Fig. 1, lower panel) and values of the gain parameters ranging from  $\sim 0.986$  to  $\sim 1.028$  for the *slope* and from  $\sim -6.6$  eV to  $\sim 8.1$  eV for the *offset*. This implies that there could be variations up to  $\sim 4\%$  of the *slope* and of  $\sim 15$  eV of the *offset*<sup>2</sup> throughout the  $\sim 10$  years and source positions sampled by the XMM-Newton observations (see Fig.

<sup>2</sup> Note that the PN channel energy has a width of  $\sim 5$  eV, which means that the photon energy as detected by the instrument is not known better than that.

**Table 1.** Log of all EPIC-pn observations of RX J1856.5-3754 performed in Small Window Mode.

Observation	Date	Obs.ID	Net Exposure Time [s]	Counts
A	2002-04-08	0106260101	40030	302601
B	2004-09-24	0165971601	22960	174955
C	2005-03-23	0165971901	14190	106949
D	2005-09-24	0165972001	22700	168609
E	2006-03-26	0165972101	48340	361845
F	2006-10-24	0412600101	49820	374018
G	2007-03-14	0412600201	26940	204513
H	2007-03-25	0415180101	16540	126883
I	2007-10-04	0412600301	23920	179449
J	2008-03-13	0412600401	33080	245923
K	2008-10-04	0412600601	43580	330553
L	2009-03-19	0412600701	47510	353698
M	2009-10-07	0412600801	40780	306449
N	2010-03-22	0412600901	48380	360306
O	2010-09-29	0412601101	47870	356580
P	2011-03-14	0412601301	45210	342204
Q1	2011-10-05*	0412601501	17490	134747
Q2	"	"	16310	124431
Q2	"	"	16800	127176
Q4	"	"	17920	128549

(\*) The observation of October 2011 has been divided in 4 pointings, with the source at different positions on the detector.

3). This is a conservative estimate since we considered the two most extreme spectra and assumed no intrinsic spectral variability in J1856.

### 2.1. CONSTRAINTS ON INTRINSIC SPECTRAL VARIATIONS

To investigate possible variations of the spectral properties of J1856 during the nine year-long time-span of the monitoring campaign, we have to compare only homogeneous data sets, i.e. when the source was located at approximately the same detector coordinates, in order to reduce the incidence of the systematic uncertainty reported in the previous section.

First, we study temperature variations considering the 8 spectra of the observations with the source in the ‘soft’ region. Fitting a linear function to the derived temperatures, we obtain a negative (cooling) rate of variation of  $\sim -0.035 \pm 0.010 \text{ eV yr}^{-1}$  (Fig. 4). However, the fit is unacceptable ( $\chi^2_\nu = 5.16$  for 6 degrees of freedom) because of the first data point (observation A), which differs significantly from the others. Assuming no variations of the instrument response between April 2002 and March 2005, the ‘anomalous’ temperature inferred from the older spectrum may be explained by an intrinsic change of the source emission, like those observed in J0720, implying a relatively rapid drop in the temperature, of  $\sim 0.5 \text{ eV}$  in less than 3 years. In alternative, some subtle variations of the instrument (energy response of the pixel column) may have occurred in the same time-frame. Excluding the first data point we obtain a better fit ( $\chi^2_\nu = 1.74$  for 5 degrees of freedom) and the rate of temperature variations of  $\sim 0.023 \pm 0.015 \text{ eV yr}^{-1}$ , which is *de facto* consistent with a constant temperature at  $2\sigma$  level (Fig. 4).

If instead we use the data from the 5 ‘hard’ observations, we obtain a rate of temperature variation of  $\sim 0.044 \pm 0.026 \text{ eV yr}^{-1}$ , again consistent with a constant temperature at  $2\sigma$  level. However the value obtained is affected by larger uncertainty since, as it can be seen from the middle panel of Fig. 2, in this case there is a larger scatter of the  $kT^\infty$  values with re-

spect to those found for the ‘soft’ observations. The origin of this larger scatter is unclear and could be possibly related to a gain instability of the pixel columns within the source point spread function. In any case, owing to their homogeneity and longer total exposure, throughout the rest of the paper we will make use of only the ‘soft’ data in order to constrain the spectral properties of J1856.

### 2.2. BEYOND THE SINGLE BLACKBODY

In order to obtain a single spectrum with high statistics, we merge together the 7 spectra of the ‘soft’ group (Fig. 3) excluding, as before, the anomalous observation of April 2002 (observation A). The resulting spectrum contains  $\sim 1.9 \times 10^6$  background-subtracted counts and corresponds to a net integration time of  $\sim 254$  kiloseconds.

We first try fits with a single BB (Fig. 5, upper panel). In order to obtain a formally acceptable fit (null hypothesis probability  $> 0.1$ ) we add a systematic error of 1.5% (*systematic* parameter in XSPEC). This is an energy-independent systematic error added to the model in XSPEC and accounts for the uncertainties on the spectral model and for likely residual calibration inaccuracies. We obtain a reduced  $\chi^2_\nu = 1.12$  for 176 degrees of freedom. The resulting temperature is  $kT^\infty = 61.5 \pm 0.1 \text{ eV}$ , to which corresponds an emission radius  $R^\infty = 5.0 \pm 0.1 \text{ km}$  for a distance of 120 pc. The column density is  $N_H = (4.8 \pm 0.2) \times 10^{19} \text{ cm}^{-2}$ . The fit residuals exhibit systematic deviations both at the lowest and highest ends of the energy range (Fig. 5, upper panel), which may be indicative of the inability of the single temperature BB to adequately fit the spectrum of J1856.

The presence of a second BB at different temperature is expected to explain pulsations (e.g. Tiengo & Mereghetti, 2007). We therefore fit the merged spectrum with a two BB model (Fig. 5, lower panel). In this case we obtain an acceptable fit by adding a systematic error of 0.6%, which returns a  $\chi^2_\nu = 1.11$ . The column density is now  $N_H = (12.9 \pm 2.2) \times 10^{19} \text{ cm}^{-2}$ . The hard BB has a temperature of  $kT_h^\infty = 62.4^{+0.6}_{-0.4} \text{ eV}$  with emis-

sion radius of  $R_h^\infty = 4.7_{-0.3}^{+0.2} (d/120 \text{ pc}) \text{ km}$ , while the soft BB has a temperature  $kT_s^\infty = 38.9_{-2.9}^{+4.9} \text{ eV}$  and emission radius  $R_s^\infty = 11.8_{-0.4}^{+5.0} (d/120 \text{ pc}) \text{ km}$ . We summarize these results in Table 2. Interestingly, the contribution of both the soft and hard X-ray blackbodies to the optical flux can account for the excess observed in J1856 (van Kerkwijk & Kulkarni, 2001; Kaplan et al., 2011). Considering the best-fit parameters for the double BB model, the contribution of the soft BB at optical wavelengths is  $\sim 4$  times larger than that of the hard BB. This implies an overall increase of a factor  $\sim 5$  with respect to the optical flux expected from the Rayleigh-Jeans tail of the hard BB alone (Fig. 6). This value is consistent, within uncertainties, to the factor  $\sim 7$  obtained from the comparison between optical/UV photometry and the extrapolation of the X-ray data (Burwitz et al., 2003; Kaplan et al., 2011).

We note three dips at  $\sim 0.3, 0.4$  and  $0.6 \text{ keV}$  in the residuals of both single and two-component BB fits. Since their width is smaller than the energy resolution of the pn detector in the range of interest, they are most likely due to non perfect instrumental calibrations, as already suggested by Haberl (2007). We search for other possible features in the spectrum of J1856, adopting the single BB model with no systematic errors in order to facilitate the comparison with the spectral features found in other XDINS. We investigate the presence of narrow absorption features from 300 to 700 eV at 100 eV intervals. We use the gaussian model from the XSPEC library, imposing fixed line energy and width<sup>3</sup> ( $\sigma = 0$  in XSPEC) and negative normalization. We find a feature at 400 eV, most likely one of the aforementioned dips and therefore of instrumental origin, with equivalent width of  $2.0 \pm 0.5 \text{ eV}$  at  $4\sigma$  confidence. No other narrow features are found at the same confidence level, corresponding to a maximum equivalent width of  $\sim 6 \text{ eV}$ . Typically, XDINSs exhibit broad absorption lines. Hence, we look for broad features (fixed line width  $\sigma = 0.1 \text{ keV}$ ) but with line energy free to vary. We find a feature at  $370 \pm 15 \text{ eV}$  and equivalent width  $9 \pm 2 \text{ eV}$  at  $4\sigma$  confidence. However, the reality of this line is debatable and could arise from an attempt to fit a non purely Planckian spectral continuum. In fact, if we adopt the two-component BB as starting model, no broad features are found at  $4\sigma$  confidence level.

### 3. DISCUSSION

A spectral analysis of all the imaging observations of the isolated neutron star RX J1856.5-3754, performed from 2002 to 2011 with the EPIC-pn instrument on-board the XMM-Newton satellite, revealed small amplitude variations, of the order of  $\sim 1-2\%$ , quantified by changes in the fit parameters obtained with a single absorbed BB model. The long term trend of these variations suggested an instrumental origin, since there is a correlation of the fit parameters with the position of the source image on the detector. This is likely related to a non-uniform energy response between different channels of the readout electronics. The related uncertainty has been quantified with a gain fit in XSPEC, resulting in variations of the gain *slope* and *offset* of  $\sim 4\%$  and  $\sim 15 \text{ eV}$ , respectively, over the pn detector positions covered by the J1856 observations (Fig. 3).

Using only homogeneous data, we found that the rate of temperature variations, in the framework of the single BB model, is compatible with a constant at  $2\sigma$  confidence level over the last

$\sim 5$  years of the monitoring campaign. A higher temperature was recorded on April 2002. If not caused by subtle alterations of the instrument response, this difference would imply that also J1856 undergoes spectral changes, albeit the magnitude of these changes is much smaller than that observed in J0720. The observed temperature changed of  $\sim 0.5 \text{ eV}$  in three years (or less, considering the lack of coverage between April 2002 and March 2005) corresponds to a rate of  $\sim -0.15 \text{ eV yr}^{-1}$ . In any case, the long term behavior of J1856 is markedly different from that of J0720. The latter underwent substantial and continuous changes in its observed spectral properties during the years. Apart the slightly higher temperature recorded in April 2002, J1856 exhibits instead a steady behavior, with no spectral variations in the last 5 years.

By merging all the homogeneous data-sets we obtained a high statistics spectrum with which we tested the validity of single and two BB models and checked for the presence of features in the spectrum of J1856. Apart some narrow features likely due to calibration issues and already reported in the literature (Haberl, 2007), we found no convincing evidence for broad or narrow absorption features. The absence of lines thus remains one of the distinctive properties of J1856 among XDINSs (see also Hohle et al., 2011). The two BB model returns a better fit to the data and is more physically justified by the observed pulsations. The presence of a second, cooler BB component was invoked by Pons et al. (2002) to explain the optical/UV data but its contribution to the X-ray flux was considered negligible because of the apparent lack of pulsations reported for J1856 at that time (Braje & Romani, 2002; Burwitz et al., 2003; Trümper et al., 2004). This implied an upper limit on the temperature of the cold BB,  $kT_{opt}^\infty < 33 \text{ eV}$ , which in turn yielded a lower limit on the stellar radius,  $R^\infty = ((R_{opt}^\infty)^2 + (R_X^\infty)^2)^{1/2} > 16 (d/120 \text{ pc}) \text{ km}$ . An even larger value was found by Hambaryan et al. (2011) for RBS 1223 (1RXS J130848.6+212708), another XDINS. It must be noted however that they assumed a condensed surface with a thin hydrogen atmosphere model to fit the spectrum of this neutron star. Thus, the measure of the radius resulting from the fit is larger than that obtained with a BB spectrum. From our analysis we found instead a smaller radius,  $R^\infty = ((R_s^\infty)^2 + (R_h^\infty)^2)^{1/2} = 12.7_{-0.2}^{+4.6} (d/120 \text{ pc}) \text{ km}$ , consistent at  $1\sigma$  level with the lower limit reported by Trümper et al. Thus, our result allows a wider

**Table 2.** Summary of fit parameters for the joint spectrum.

Parameter	Single BB	Two BB
$N_H$ [ $10^{19} \text{ cm}^{-2}$ ]	$4.8_{-0.2}^{+0.2}$	$12.9_{-2.3}^{+2.2}$
$kT_h^\infty$ [eV]	$61.5_{-0.1}^{+0.1}$	$62.4_{-0.4}^{+0.6}$
$R_h^\infty$ [km]	$5.0_{-0.1}^{+0.1}$	$4.7_{-0.3}^{+0.2}$
$kT_s^\infty$ [eV]	-	$38.9_{-2.9}^{+4.9}$
$R_s^\infty$ [km]	-	$11.8_{-0.4}^{+5.0}$
$\sigma_{\text{sys}}$	1.5%	0.6%
$\chi^2_\nu$	1.12	1.11

<sup>3</sup> The condition  $\sigma = 0$  implies that the line width is smaller than the energy resolution. The width  $\sigma$  is thus automatically adjusted to match the minimum width imposed by the instrument resolution.

range of radii and is not much constraining for the EOS. In any case, we stress that the inferred parameters of a second BB in the X-ray spectrum of J1856 must be taken with caution. In addition to the statistical and systematic errors reported above, the normalization and thus the radius of soft BB component is affected by systematic uncertainties because of the not well constrained energy redistribution below  $\sim 0.4$  keV. Large systematic deviations are expected also because J1856 is one of the main calibration targets used to determine the instrumental energy response and so the pn response matrix is currently tuned to reproduce a X-ray spectrum of J1856 not in contrast with its optical/UV flux, if a double BB models is assumed. With the caveat of the aforementioned uncertainties, the extrapolation of the cold BB accounts also for a large fraction of the reported optical excess (e.g. Kaplan et al., 2011), avoiding the need for more complex models proposed to explain the observed optical/UV flux.

#### 4. CONCLUSIONS

The results presented in this work show that the small amplitude variations in the spectral parameters of the isolated neutron star RX J1856.5-3754, obtained by fitting its spectrum with a single absorbed BB model, are due to a non-uniform energy response of the EPIC-pn camera. Once this instrumental effect is taken into account, the upper limits on the relative temperature and flux variations in the period March 2005-present are  $\Delta kT^\infty < 0.5\%$  and  $\Delta f_X < 3\%$ , respectively. These can be taken as a measure of the source+instrument long term stability. A higher temperature was instead observed in April 2002. If due to an intrinsic change of the source spectral properties, it would imply that variations on time-scales of years, like those observed in the other XDINS RX J0720.4-3125, might be a common feature of this class of sources.

We point out that, being the two brightest and most observed XDINSs, a continuous monitoring of these two sources will help to characterize the differences and analogies in their long term behavior and thus will give insights about the physical conditions on their surfaces, like e.g. the magnetic field and temperature distributions. In the case of J1856, the steady emission allowed us to sum all the data taken with the source in the same position on the detector, in order to obtain a spectrum with high count statistics. The resulting spectrum is best fitted by a two BB model, which is also more justified than a single BB by the observation of pulsations at X-ray energies. Also, the extrapolation at optical wavelengths of the emission from the two BBs accounts for the excess reported in the literature. However, due to uncertainties in the calibration of the pn at low energies, the radius of the star is not well constrained.

Finally, the results presented here suggest that J1856 is possibly the best choice as calibration source for instruments observing in the soft X-ray domain. Moreover, the EPIC-pn detector on board XMM-Newton is extremely stable over a long time-span (see above) and so, after taking into account a subtle spatial dependence of its spectral response, it can be considered as a reference instrument for the study of long term spectral variability of X-ray sources.

*Acknowledgements.* We thank the anonymous referee for the useful comments which improved the previous version of the manuscript. We also thank M. Guainazzi and K. Dennerl for carefully reading the manuscript and for helpful discussion and suggestions. The XMM-Newton project is an ESA Science Mission with instruments and contributions directly funded by ESA Member States and the USA (NASA). We acknowledge the support of ASI/INAF through grant I/009/10/0.

#### References

- Anders, E., & Grevesse, N. 1989, *Geochim. Cosmochim. Acta*, 53, 197  
 Arnaud, K. A. 1996, *Astronomical Data Analysis Software and Systems V*, 101, 17  
 Braje, T. M., & Romani, R. W. 2002, *ApJ*, 580, 1043  
 Burwitz, V., Haberl, F., Neuhäuser, R., Predehl, P., Trümper, J., & Zavlin, V. E. 2003, *A&A*, 399, 1109  
 de Vries, C. P., Vink, J., Méndez, M., & Verbunt, F. 2004, *A&A*, 415, L31  
 Haberl, F., Turolla, R., de Vries, C. P., Zane, S., Vink, J., Méndez, M., & Verbunt, F. 2006, *A&A*, 451, L17  
 Haberl, F. 2007, *Ap&SS*, 308, 181  
 Hambaryan, V., Suleimanov, V., Schwöpe, A. D., et al. 2011, *A&A*, 534, A74  
 Ho, W. C. G., Kaplan, D. L., Chang, P., van Adelsberg, M., & Potekhin, A. Y. 2007, *MNRAS*, 375, 821  
 Hohle, M. M., Haberl, F., Vink, J., Turolla, R., Hambaryan, V., Zane, S., de Vries, C. P., & Méndez, M. 2009, *A&A*, 498, 811  
 Hohle, M. M., Haberl, F., Vink, J., Turolla, R., Zane, S., de Vries, C. P., & Méndez, M. 2010, *A&A*, 521, A11  
 Hohle, M. M., Haberl, F., Vink, J., de Vries, C. P., & Neuhäuser, R. 2011, *arXiv:1109.2506*  
 Kaplan, D. L., & van Kerkwijk, M. H. 2005, *ApJ*, 628, L45  
 Kaplan, D. L., van Kerkwijk, M. H., & Anderson, J. 2007, *ApJ*, 660, 1428  
 Kaplan, D. L., Kamble, A., van Kerkwijk, M. H., & Ho, W. C. G. 2011, *arXiv:1105.4178*  
 Lai, D. 2001, *Reviews of Modern Physics*, 73, 629  
 Mereghetti, S. 2008, *A&A Rev.*, 15, 225  
 Pons, J. A., Walter, F. M., Lattimer, J. M., et al. 2002, *ApJ*, 564, 981  
 Pons, J. A., Miralles, J. A., & Geppert, U. 2009, *A&A*, 496, 207  
 Read, A. M., Sembay, S. F., Abbey, T. F., & Turner, M. J. L. 2006, *The X-ray Universe 2005*, 604, 925  
 Strüder, L., et al. 2001, *A&A*, 365, L18  
 Stuhlinger, M., et al. 2011, "Status of the XMM-Newton Cross-calibration with SASv10.0" (<http://xmm2.esac.esa.int/docs/documents/CAL-TN-0052.ps.gz>)  
 Tiengo, A., & Mereghetti, S. 2007, *ApJ*, 657, L101  
 Trümper, J. E., Burwitz, V., Haberl, F., & Zavlin, V. E. 2004, *Nuclear Physics B Proceedings Supplements*, 132, 560  
 Turolla, R., Zane, S., & Drake, J. J. 2004, *ApJ*, 603, 265  
 Turolla, R. 2009, *Astrophysics and Space Science Library*, 357, 141  
 van Kerkwijk, M. H., & Kulkarni, S. R. 2001, *A&A*, 378, 986  
 van Kerkwijk, M. H., Kaplan, D. L., Pavlov, G. G., & Mori, K. 2007, *ApJ*, 659, L149  
 van Kerkwijk, M. H., & Kaplan, D. L. 2008, *ApJ*, 673, L163  
 Vink, J., de Vries, C. P., Méndez, M., & Verbunt, F. 2004, *ApJ*, 609, L75  
 Yakovlev, D. G., Ho, W. C. G., Shternin, P. S., Heinke, C. O., & Potekhin, A. Y. 2011, *MNRAS*, 411, 1977  
 Walter, F. M., Wolk, S. J., & Neuhäuser, R. 1996, *Nature*, 379, 233  
 Walter, F. M., & Lattimer, J. M. 2002, *ApJ*, 576, L145  
 Walter, F. M., Eisenbeiß, T., Lattimer, J. M., et al. 2010, *ApJ*, 724, 669

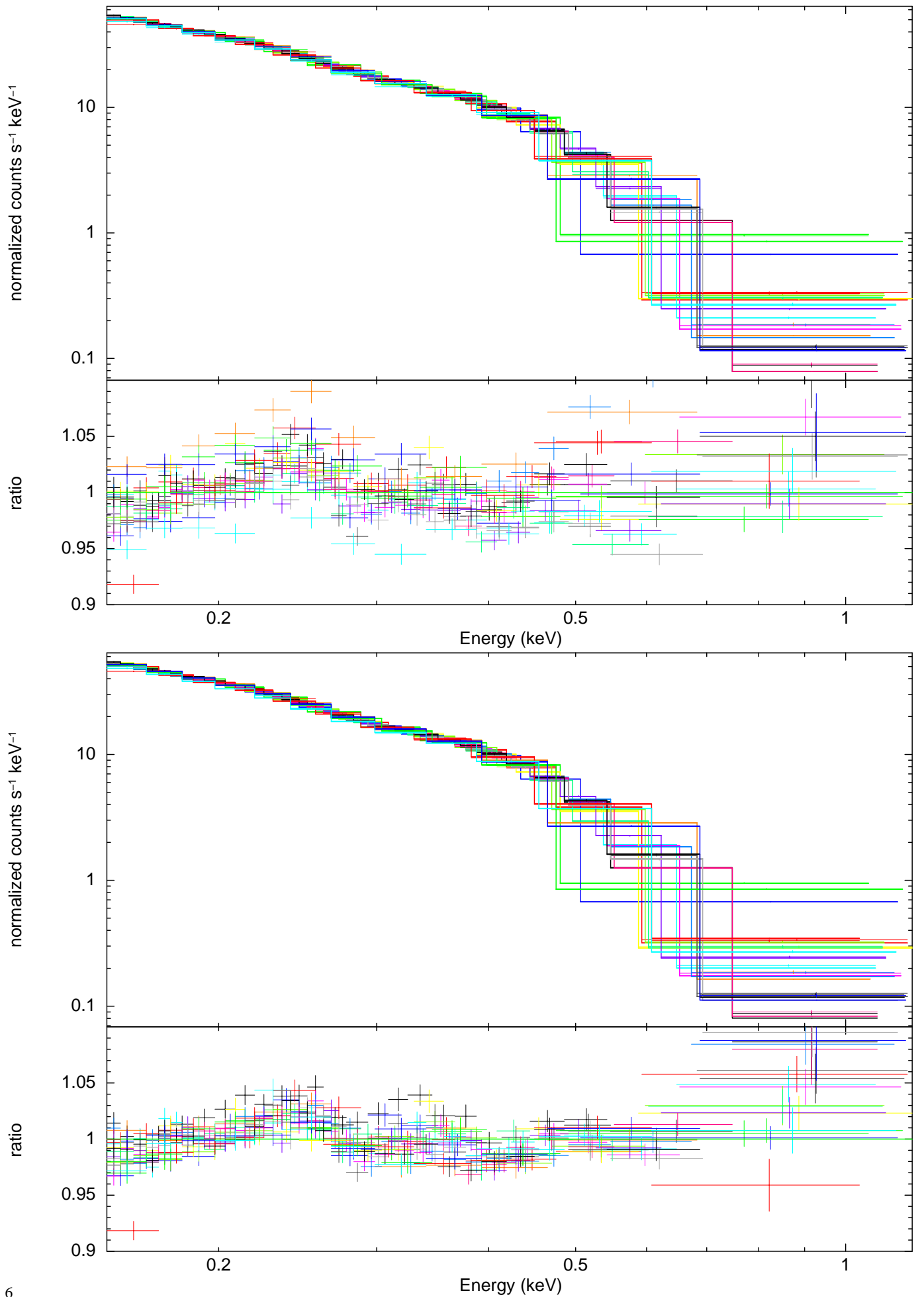


**Fig. 1.** Simultaneous fit of all J1856 spectra with the same single BB. Upper (lower) panel shows the residuals without (with) the gain parameters free to vary.

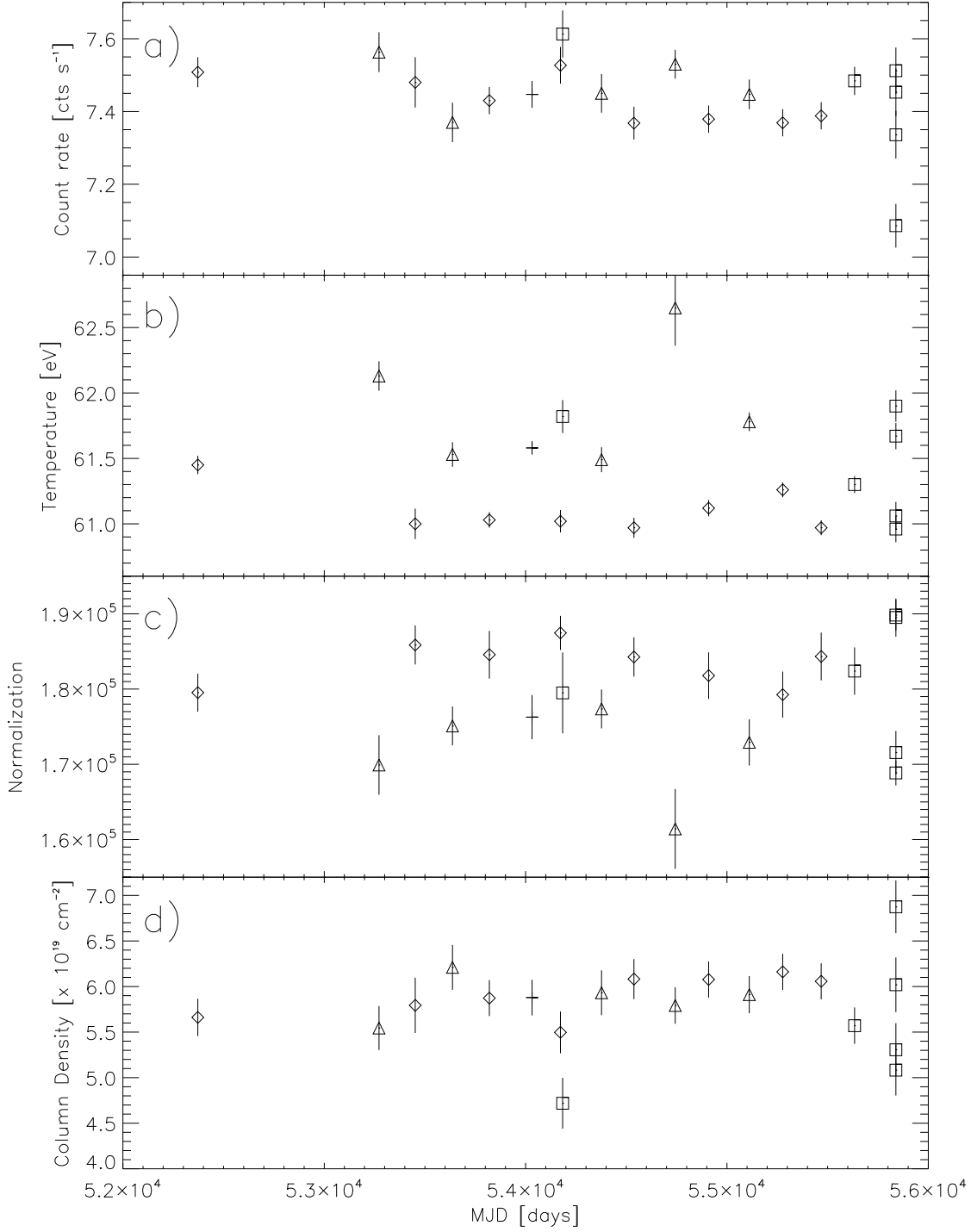


**Fig. 2.** Long term evolution of the spectral parameters obtained with a single BB fit in the 0.15 – 1.2 keV range. Panels *a*, *b*, and *c*, show the count rate, temperature, and BB normalization of a simultaneous fit with the column density fixed to a common value. Panel *d* indicates the column density obtained when, instead, the BB parameters are fixed to a common value for all the observations (see text). Diamonds, triangles and squares represent ‘soft’, ‘hard’ and off-axis observations, respectively. The plus symbol is the October 2006 observation, which is at an intermediate detector position (see Fig. 3). Error bars correspond to  $3\sigma$  confidence intervals.

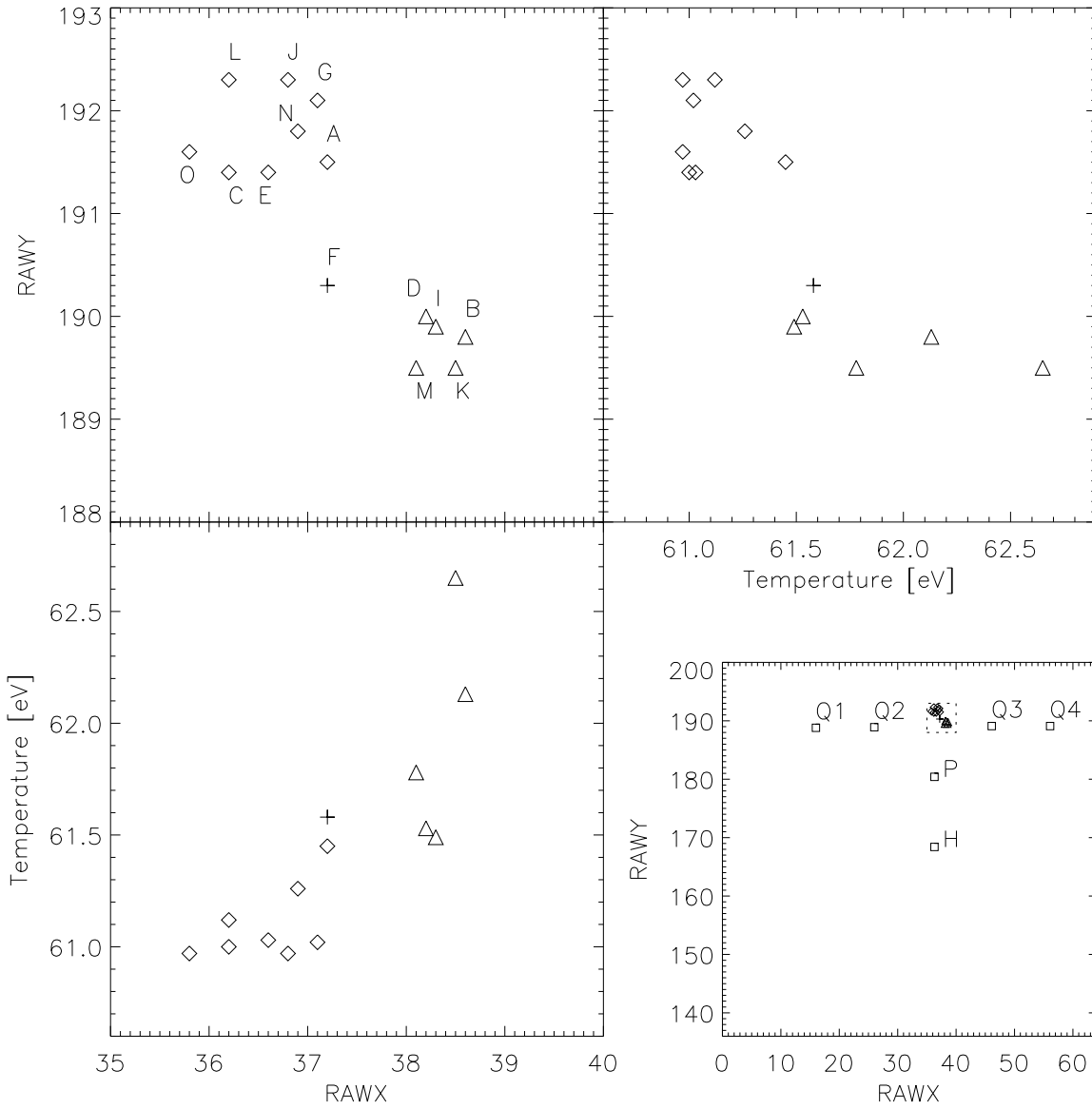


**Fig. 3.** Lower right panel: position of the source in detector coordinates (RAWX,RAWY). The region in the dashed square is enlarged in the upper left panel. The symbols indicate the different observations: ‘soft’ region (diamonds), ‘hard’ region (triangles), observation F (plus), off-axis observations (squares). The other two panels indicate the temperature as a function of the source position.



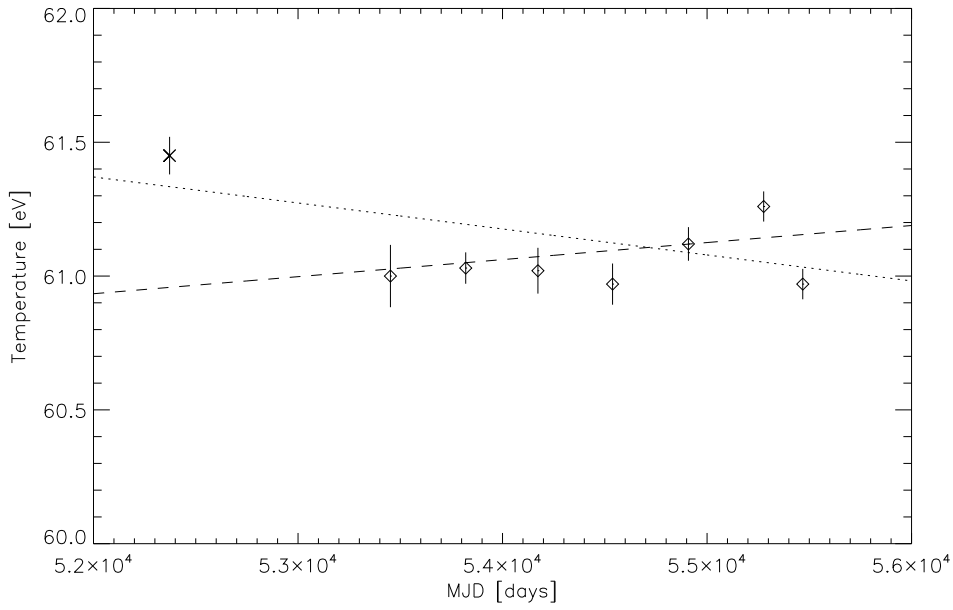


**Fig. 4.** Long term evolution of the temperature for ‘soft’ observations. The dotted line represents the linear fit to the data. The dashed line represents a linear fit to the data without considering the observation of April 2002, which is marked by the X symbol. Error bars correspond to  $3\sigma$  confidence intervals.

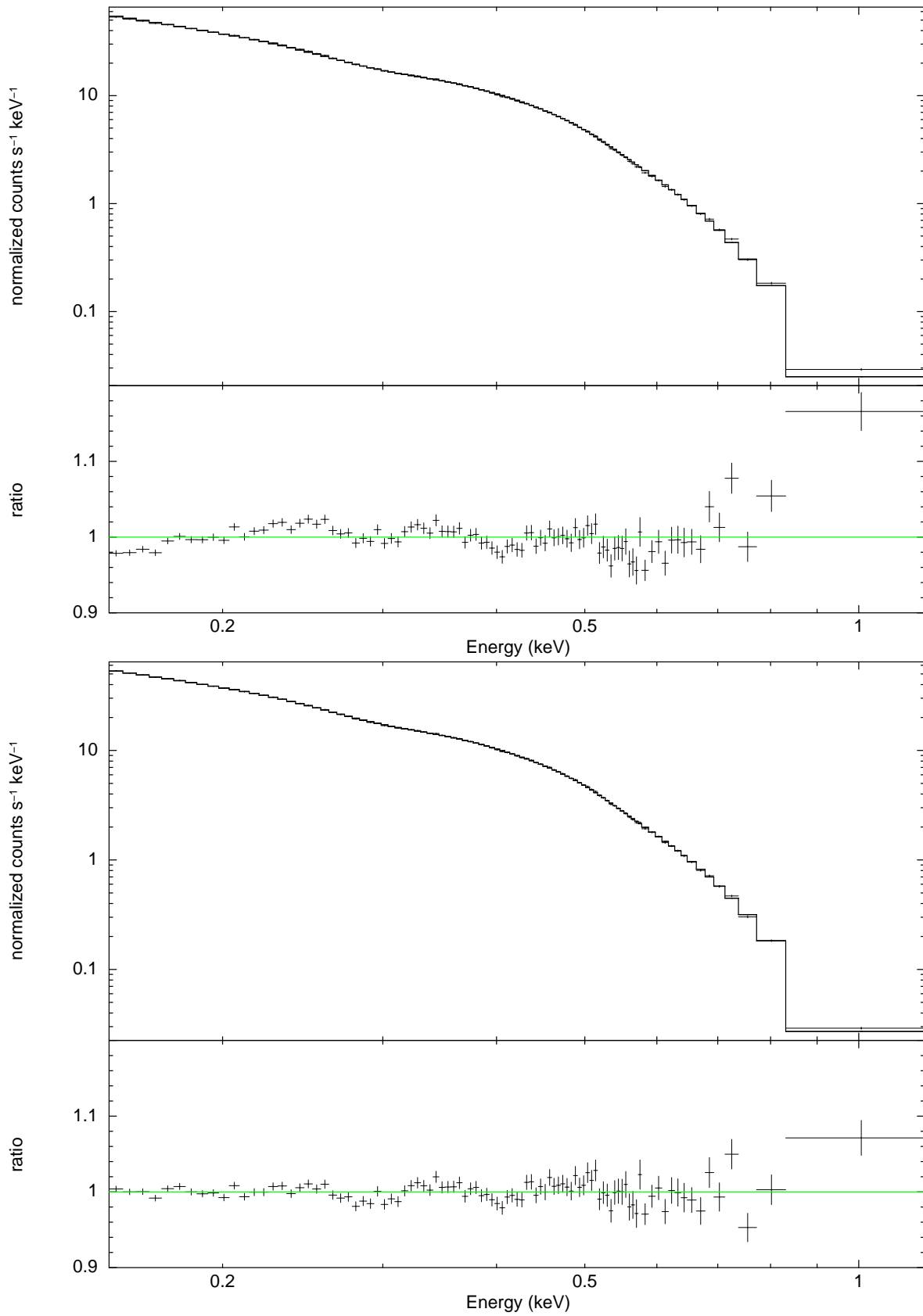


**Fig. 5.** (Top) Single BB fit of the merged spectrum obtained from observations of the 'soft' group. (Bottom) Same as Top panel but with a two BB model.

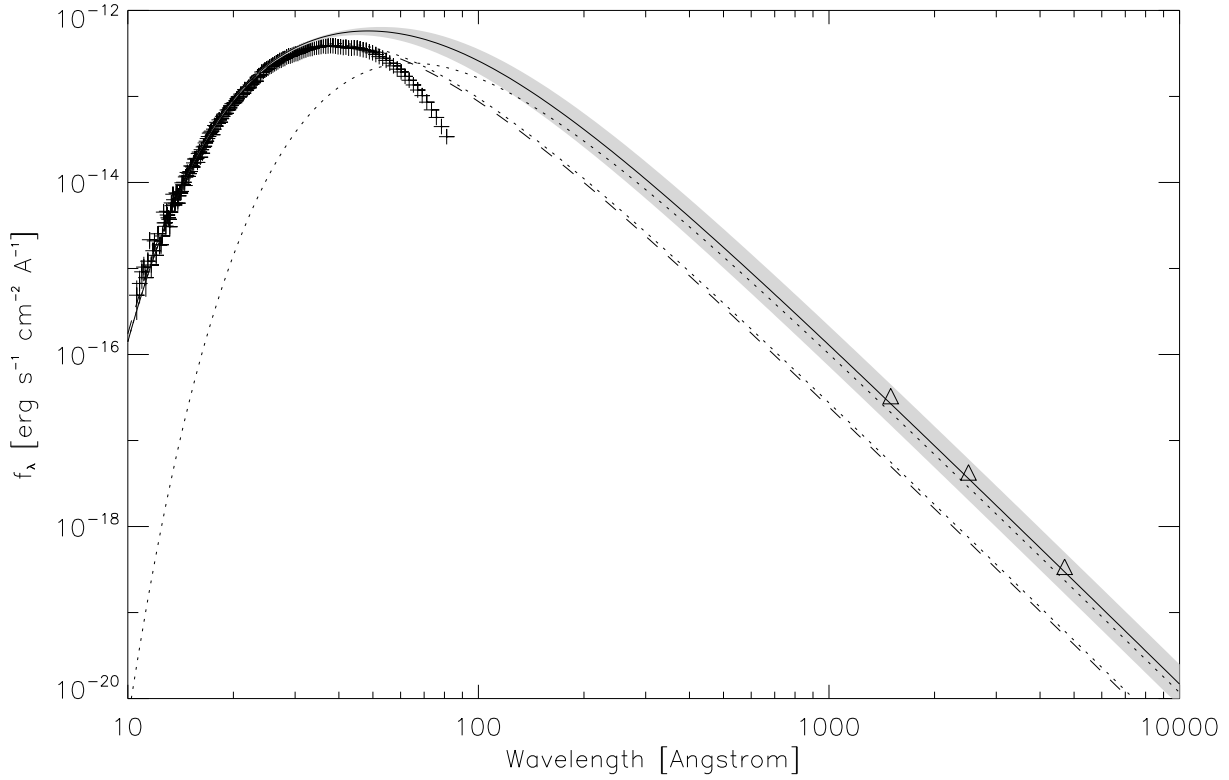


**Fig. 6.** Broadband spectrum of J1856. The dashed line is the extrapolation of the (unabsorbed) X-ray BB from Burwitz et al. (2003). The dotted lines indicate the two BB components obtained from the sum of all the homogeneous observations with the source in the ‘soft’ region, and the solid line is their sum. The shaded area marks the  $1\sigma$  confidence region for the best fit model. The triangles represent the optical/UV data obtained from HST photometry (Kaplan et al., 2011).